A Novel Semi-Analytical Approach for Fast Electromigration Stress Analysis in Multi-Segment Interconnects

Olympia Axelou
oaxelou@e-ce.uth.gr
University of Thessaly
Volos, Greece

Nestor Evmorfopoulos
nestevmo@e-ce.uth.gr
University of Thessaly
Volos, Greece

George Floros
gefloros@e-ce.uth.gr
University of Thessaly
Volos, Greece

George Stamoulis
georges@e-ce.uth.gr
University of Thessaly
Volos, Greece

Sachin S. Sapatnekar
sachin@umn.edu
University of Minnesota
Minneapolis, MN, US

ABSTRACT

As integrated circuit technologies move below 10 nm, Electromigration (EM) has become an issue of great concern for the longterm reliability due to the stricter performance, thermal and power requirements. The problem of EM becomes even more pronounced in power grids due to the large unidirectional currents flowing in these structures. The attention for EM analysis during the past years has been drawn to accurate physics-based models describing the interplay between the electron wind force and the back stress force, in a single Partial Differential Equation (PDE) involving wire stress. In this paper, we present a fast semi-analytical approach for the solution of the stress PDE at discrete spatial points in multi-segment lines of power grids, which allows the analytical calculation of EM stress independently at any time in these lines. Our method exploits the specific form of the discrete stress coefficient matrix whose eigenvalues and eigenvectors are known beforehand. Thus, a closed-form equation can be constructed with almost linear time complexity without the need of time discretization. This closed-form equation can be subsequently used at any given time in transient stress analysis. Our experimental results, using the industrial IBM power grid benchmarks, demonstrate that our method has excellent accuracy compared to the industrial tool COMSOL while being orders of magnitude times faster.

CCS CONCEPTS

• **Hardware** → *Physical design (EDA)*; **Aging of circuits and systems**.

KEYWORDS

Longterm Reliability, Electromigration, Stress Diffusion, Korhonen's PDE, Analytical Solution

ICCAD '22, October 30-November 3, 2022, San Diego, CA, USA

ACM ISBN 978-1-4503-9217-4/22/10…$15.00
https://doi.org/10.1145/3508352.3549476

ACM Reference Format:
Olympia Axelou, Nestor Evmorfopoulos, George Floros, George Stamoulis, and Sachin S. Sapatnekar. 2022. A Novel Semi-Analytical Approach for Fast Electromigration Stress Analysis in Multi-Segment Interconnects. In *IEEE/ACM International Conference on Computer-Aided Design (ICCAD '22), October 30-November 3, 2022, San Diego, CA, USA.* ACM, New York, NY, USA, 7 pages. https://doi.org/10.1145/3508352.3549476

1 INTRODUCTION

Electromigration (EM) has become a great concern for the semiconductor industry in recent years. EM failures are an inevitable consequence of the rising current demands and the technology downscaling, which can lead to several open- or short-circuits in the metal interconnects on the chip [1, 2]. The above has made EM analysis an integral part of modern VLSI design methodologies [3].

Traditional EM analysis approach is composed by a two-stage process, the application of the Blech criterion [4] and then the Black's equation [5]. The first formula serves in distinguishing the "immortal" lines from the ones that will potentially encounter an EM failure. For the rest of the lines, that are not considered EM safe, Black's equation predicts their mean time to failure. However, these methods are heuristic in nature and, having been developed for older technologies, are shown to be inaccurate for proper EM analysis in modern chips [6].

Contrary to the above empirical methods, Korhonen et al. [7] have developed an exact physics-based model which is expressed as a diffusion-type partial differential equation (PDE) for each segment of a metal interconnect. The resulting model describes the interaction between the wind force of the electron momentum and the compressive stress force created by the accumulation of metal atoms, in a single PDE involving stress and expressing its temporal evolution along the wire. Several EM stress analysis methodologies based on the solution of Korhonen's equation, have focused on calculating the steady-state stress [8] when equilibrium is reached along the wire. Then a wire segment is deemed as "immortal" if its steady-state stress is below a critical stress value. However, the time to reach steady-state can surpass, by a large margin, the expected lifetime of the chip. In this context, transient stress analysis is useful, which calculates the temporal stress behavior during the chip lifetime. A wire segment is then considered as susceptible to EM failure only if its stress exceeds the critical value during the lifetime of the chip.

Previous approaches for computing transient stress response can be divided into two main classes. Firstly, numerical methods such as [9–11] are very popular due to their simplicity, and they are already integrated into commercial tools such as COMSOL. The main attribute of these methods is that they perform discretization of space and time, and are in principle applicable to a wide spectrum of geometries due to the spatial discretization. However, these methods come with a large performance cost due to the temporal discretization, especially for simulating typical chip lifetimes in the order of decades, since transient analysis needs to be performed point-after-point in time.

On the other hand, analytical methods for solving Korhonen's equation keep both space and time continuous, and are much better suited to large-scale systems and long chip lifetimes when they are applicable. Previous analytical approaches [12, 13] calculate infinite series solutions for very small geometries, consisting of up to four wire segments. A considerably more general analytical approach is proposed in [14], which introduces the novel concept of stress reflections and can be applied to general multi-segment lines with an arbitrary number of segments. Nevertheless, all analytical methods involve the approximation of infinite series with a finite number of terms, whose number is dependent on both line length and time and cannot be known beforehand. Another analytical approach was proposed in [15], but it also involves finite-term approximation of infinite series and also resorts to expensive numerical techniques for the calculation of eigenvalues.

In this paper, we present a novel semi-analytical approach to the solution of the KorhonenâĂŹs equation for multi-segment lines (such as typically found in power grids), which discretizes only space while keeping the time continuous. The main contributions of this paper are summarized hereafter. *First*, our method can calculate stress for any given input time, providing a simple closed-form matrix equation that can be reused for any number of input times. We note that the major benefit of keeping time continuous is allowing the calculation of stress at any time directly (especially for long chip lifetimes, which can render numerical time integration completely prohibitive), while spatial discretization is much less important because even in fully analytical methods we still compute stress at specific discrete spatial points. *Second*, in contrast to fully analytical solutions which involve approximations such as truncation of infinite series to undefined number of terms, our method does not make any approximation in the calculation of stress for the given time. *Third*, the calculation of stress for the input time is performed simultaneously at all spatial discrete points with almost linear complexity, as it involves the application of the Fast Fouier Transform (FFT) in what is essentially a variant of a Fast Poisson Solver [16]. Our experiments on industrial large-scale benchmarks prove the scalability of our method, while its efficiency is validated against COMSOL by achieving great speedups.

The rest of this paper is organized as follows. Section 2 provides a basic background on EM analysis due to void nucleation and void growth. Then, in Section 3 we present our main contributions in the analytical solution of the Korhonen's diffusion equation. Section 4 demonstrates the experimental results of the application of our method on the large-scale industrial IBM benchmarks as well as its comparison with COMSOL. Finally, Section 5 completes our study where the conclusions are drawn.

2 BACKGROUND

2.1 EM Stress Analysis on an Interconnect Line

As the current flows in the wire, two opposing forces are exerted on the metal atoms[1], the first one being an electrostatic force F_{field} which results from the electric field's effect on the atoms and points to a direction opposite to the electron flow (Fig. 1). The second force F_{wind} is generated by the momentum exchange between the conducting electrons that come into collision with the atoms and is in the same direction as the electric field. The latter is the predominant force since the electrostatic force is relatively small due to the shielding electrons [17].

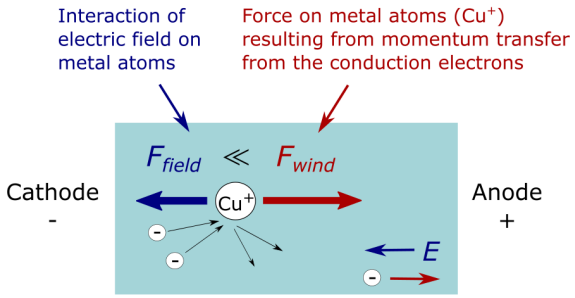

Figure 1: The two forces that act on the Cu atoms [3].

If the total force (in the direction of the wind force) exceeds the activation energy E_a, then the phenomenon of EM begins and metal atoms move towards the anode. As time passes, the change in the wire volume, as well as the enduring unidirectional current, will increase hydrostatic stress by creating tensile stress at the cathode and compressive stress at the anode of the wire. The resulting concentration gradient generates a new force, the F_{back_stress}, which acts against the electron wind force and takes the place of F_{field} since its effect becomes relatively negligible. It is important to model the results of this back-stress force since if the stress reaches a critical level, it can lead to the creation of voids (void nucleation) at the cathode of the line and hillock formation at the anode [3], which subsequently lead to open circuits and the end of the lifetime for the wire.

It is well known that for modern Cu dual damascene (Cu DD) interconnect technology, with capping and barrier layers, there is no mass transfer across layers, and all EM-induced metal migration occurs within the same layer [18]. In practical power grids, there might be very short leads, "stubs", that connect the line to vias, but they can be considered unimportant to the evolution of the phenomenon of EM. Therefore, a large interconnect system such as a power grid can be analyzed layer-by-layer. Furthermore, power grids in modern chips tend to use unidirectional routing within each layer of the mesh-like orthogonal-wire structures and can therefore be decomposed into multi-segment lines [14]. Taking the above into consideration, it suffices to examine each multi-segment line separately, thus this paper focuses on the analysis of 1D multi-segment line structures, where each segment could potentially carry a different current density.

[1]Metal *atoms* and metal *ions* are thought as equivalent in the context of this paper.

2.2 Korhonen's Model

In order to examine the stress, the most established model is the Korhonen's PDE [7], or stress diffusion equation:

$$\frac{\partial \sigma}{\partial t} = \frac{\partial}{\partial x}\left[\kappa\left(\frac{\partial \sigma}{\partial x} + \beta j\right)\right] \tag{1}$$

Here, $\beta = e\rho Z^*/\,\Omega$ and $\kappa = D_\alpha B\Omega/(k_B T)$ with $D_\alpha = D_o e^{-E_a/kT}$ being the diffusion coefficient and E_a the activation energy; j is the current density through the the specific segment of the wire, e is the electron charge, ρ is the electrical resistivity of the wire, Z^* is the effective charge number, Ω is the atomic volume for the metal; D_o is the diffusivity constant, B is the bulk modulus for the metal, k_B is the Boltzmann's constant and T is the temperature; t is time and x is the spatial coordinate.

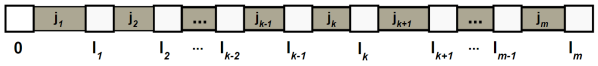

Figure 2: An m-segment interconnect line.

A multi-segment interconnect line consists of line segments with different current densities that are separated by vias. For an m-segment interconnect line, shown in Fig. 2, Korhonen's equation (1) holds in each segment $k = 1, \ldots, m$ of the line. This is supplemented by the following boundary conditions (BCs), which must hold for all time points [19]:

BC 1. At the terminal points $x = 0$ (cathode) and $x = l_m$ (anode), the atomic flux must be zero:

$$\left(\frac{\partial \sigma}{\partial x}\bigg|_{x=0} + \beta j_1\right) = 0\,, \quad \left(\frac{\partial \sigma}{\partial x}\bigg|_{x=l_m} + \beta j_m\right) = 0 \tag{2}$$

BC 2. At the intersection l_k between segments k and $k+1$, the atomic flux must be continuous:

$$\left(\frac{\partial \sigma_k}{\partial x}\bigg|_{x=l_k} + \beta j_k\right) = \left(\frac{\partial \sigma_{k+1}}{\partial x}\bigg|_{x=l_k} + \beta j_{k+1}\right) \tag{3}$$

BC 3. At the intersection l_k between segments k and $k+1$, the stress itself must be continuous:

$$\sigma_k\big|_{x=l_k} = \sigma_{k+1}\big|_{x=l_k} \tag{4}$$

2.3 Spatial Discretization of the wire

In this subsection, we apply the finite-difference method (FDM) to discretize the spatial derivative in Korhonen's equation (1), in order to obtain a system of ordinary differential equations (ODEs) for the multi-segment wire.

Let n be the number of discretization points along the spatial coordinate x. Typically each of the m wire segments in Fig. 2 will be discretized into one or more elements, so that $n \geq m$. As an example, we see in Fig. 3 a two-segment line that is discretized with a spatial step Δx into six discrete points: two zero-flux terminal points, one via intersection point, and three internal points. As can be seen in the figure, there are also two more discretization points outside the geometry, which are solely used for the formulation of the FDM equations for the terminal (zero-flux) points.

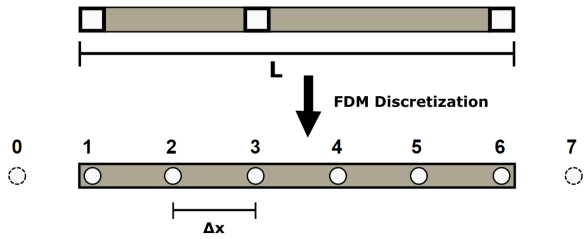

Figure 3: Spatial discretization of a two-segment wire.

By applying a finite difference approximation of the spatial derivative in (1), we get for every discretized point $i = 1, \ldots, n$ of the wire:

$$\begin{aligned}\frac{\partial \sigma_i}{\partial t} \equiv \dot{\sigma}_i &= \kappa \frac{\left(\frac{\sigma_{i+1}-\sigma_i}{\Delta x}\right) - \left(\frac{\sigma_i - \sigma_{i-1}}{\Delta x}\right)}{\Delta x} \\ &= \frac{\kappa}{\Delta x^2}\left(\sigma_{i+1} - 2\sigma_i + \sigma_{i-1}\right)\end{aligned} \tag{5}$$

The FDM approximations for the endpoints of the multi-segment wire are obtained by eliminating, in (5), the non-physical points that are outside the geometry, through the zero-flux BCs (2). For the cathode we apply the backward difference:

$$\frac{\sigma_1 - \sigma_0}{\Delta x} + \beta j_1 = 0 \tag{6}$$

while for the anode we use the forward difference:

$$\frac{\sigma_{n+1} - \sigma_n}{\Delta x} + \beta j_m = 0 \tag{7}$$

Note that the spatial derivatives in (2) are approximated in the direction of increasing x (the convention used in [7] is that x increases in the direction of electron current, i.e. opposite to the conventional current). By applying (5) for $i = 1$ and $i = n$, and eliminating σ_0 and σ_{n+1} from (6) and (7) respectively, we arrive at the FDM equations for σ_1 and σ_n:

$$\begin{aligned}\dot{\sigma}_1 &= \frac{\kappa}{\Delta x^2}\left(\sigma_2 - \sigma_1\right) + \frac{\kappa}{\Delta x}\beta j_1 \\ \dot{\sigma}_n &= \frac{\kappa}{\Delta x^2}\left(-\sigma_n + \sigma_{n-1}\right) - \frac{\kappa}{\Delta x}\beta j_m\end{aligned} \tag{8}$$

For the via intersection points, the FDM approximation results by spatially discretizing (1) and applying the continuous-flux BCs (3). Specifically for the point connecting segments k and $k+1$, the FDM approximation is:

$$\dot{\sigma}_i = \frac{\kappa}{\Delta x^2}\left(\sigma_{i-1} - 2\sigma_i + \sigma_{i+1}\right) + \frac{\kappa}{\Delta x}\beta(j_{k+1} - j_k) \tag{9}$$

Writing the FDM approximation for all discrete points from (5), (8), and (9), we arrive at the following system of ODEs:

$$\begin{bmatrix}\dot{\sigma}_1 \\ \dot{\sigma}_2 \\ \vdots \\ \dot{\sigma}_{n-1} \\ \dot{\sigma}_n\end{bmatrix} = \frac{\kappa}{\Delta x^2}\begin{bmatrix}-1 & 1 & 0 & \cdots & 0 & 0 \\ 1 & -2 & 1 & \cdots & 0 & 0 \\ \vdots & \vdots & \ddots & \ddots & \vdots & \vdots \\ 0 & 0 & \cdots & 1 & -2 & 1 \\ 0 & 0 & \cdots & 0 & 1 & -1\end{bmatrix}\begin{bmatrix}\sigma_1 \\ \sigma_2 \\ \vdots \\ \sigma_{n-1} \\ \sigma_n\end{bmatrix} + \frac{\kappa\beta}{\Delta x}\mathbf{D}\begin{bmatrix}j_1 \\ \vdots \\ j_m\end{bmatrix} \tag{10}$$

where $\mathbf{D}$ is an $n \times m$ matrix with elements $d_{11} = 1$, $d_{nm} = -1$, and $d_{ik} = -1$, $d_{i,k+1} = 1$ for the discrete points i that connect segments k and $k+1$ (and zeros everywhere else). For example, the matrix $\mathbf{D}$ for the six-point two-segment wire of Fig. 3 is:

$$\mathbf{D} = \begin{bmatrix} 1 & 0 \\ 0 & 0 \\ -1 & 1 \\ 0 & 0 \\ 0 & 0 \\ 0 & -1 \end{bmatrix} \tag{11}$$

3 ANALYTICAL SOLUTION OF TRANSIENT STRESS VIA EIGENDECOMPOSITION

The ODE system (10) has the familiar form of a linear time-invariant (LTI) system:

$$\dot{\boldsymbol{\sigma}}(t) = \mathbf{A}\boldsymbol{\sigma}(t) + \mathbf{B}\mathbf{j} \tag{12}$$

with $\mathbf{B} = \frac{\kappa\beta}{\Delta x}\mathbf{D}$ and:

$$\mathbf{A} = \frac{\kappa}{\Delta x^2}\begin{bmatrix} -1 & 1 & 0 & \cdots & 0 & 0 \\ 1 & -2 & 1 & \cdots & 0 & 0 \\ \vdots & \vdots & \ddots & \ddots & \vdots & \vdots \\ 0 & 0 & \cdots & 1 & -2 & 1 \\ 0 & 0 & \cdots & 0 & 1 & -1 \end{bmatrix} \tag{13}$$

The analytical solution of (12) can be obtained as the convolution integral [20]:

$$\boldsymbol{\sigma}(t) = e^{\mathbf{A}t}\boldsymbol{\sigma}(0) + \int_0^t e^{\mathbf{A}(t-\tau)}\,\mathbf{B}\mathbf{j}\,d\tau \tag{14}$$

where $\boldsymbol{\sigma}(0)$ is the vector of initial stress conditions at the n discretized points. We note that due to nonuniform coefficients of thermal expansion of the materials, there can exist a residual thermal stress $\sigma_{T,i}$ at every point i of the line, which constitutes the initial stress condition at i. However, and without loss of generality, we can assume the absence of residual thermal stress so that the initial stress is set to $\boldsymbol{\sigma}(0) = \mathbf{0}$ everywhere.

If $\mathbf{A} = \mathbf{V}\boldsymbol{\Lambda}\mathbf{V}^{-1}$ is the eigendecomposition of $\mathbf{A}$, then it is well-known [20] that $e^{\mathbf{A}t} = \mathbf{V}e^{\boldsymbol{\Lambda}t}\mathbf{V}^{-1}$, and thus (14) becomes (for $\boldsymbol{\sigma}(0) = \mathbf{0}$):

$$\boldsymbol{\sigma}(t) = \int_0^t \mathbf{V}e^{\boldsymbol{\Lambda}(t-\tau)}\mathbf{V}^{-1}\mathbf{B}\mathbf{j}\,d\tau = \mathbf{V}\left(\int_0^t e^{\boldsymbol{\Lambda}(t-\tau)}\,d\tau\right)\mathbf{V}^{-1}\mathbf{B}\mathbf{j} \tag{15}$$

Since $\boldsymbol{\Lambda}$ is diagonal, the matrix integral in the above equation has the form:

$$\int_0^t e^{\boldsymbol{\Lambda}(t-\tau)}\,d\tau = \begin{bmatrix} \int_0^t e^{\lambda_1(t-\tau)}\,d\tau & & \\ & \ddots & \\ & & \int_0^t e^{\lambda_n(t-\tau)}\,d\tau \end{bmatrix} \tag{16}$$

where $\lambda_j, j = 1, \ldots, n$ are the (not generally distinct) eigenvalues of $\mathbf{A}$. Each of the above integrals can be computed analytically as:

$$\int_0^t e^{\lambda_j(t-\tau)}\,d\tau = \left[-\frac{e^{\lambda_j(t-\tau)}}{\lambda_j}\right]_{\tau=0}^{\tau=t} = \frac{e^{\lambda_j t} - 1}{\lambda_j} \tag{17}$$

Note that if one eigenvalue equals zero, then the corresponding integral is simply $\int_0^t d\tau = t$.

Now, for the specific matrix $\mathbf{A}$ with the form (13), it was shown in [21] that its eigendecomposition can be determined beforehand. Specifically, $\mathbf{A}$ has n distinct eigenvalues which are given by:

$$\lambda_j = \frac{\kappa}{\Delta x^2}\left(2\cos\frac{(j-1)\pi}{n} - 2\right), \quad j = 1, \ldots, n \tag{18}$$

along with n orthonormal eigenvectors (such that $\mathbf{V}^{-1} = \mathbf{V}^T$) with elements:

$$v_{i,j} = \begin{cases} \sqrt{\frac{1}{n}}, & j = 1 \\ \sqrt{\frac{2}{n}}\cos\frac{(2i-1)(j-1)\pi}{2n}, & j = 2, \ldots, n \end{cases} \quad i = 1, \ldots, n \tag{19}$$

Moreover (and more importantly), the products $\mathbf{V}^T\mathbf{r}$ and $\mathbf{V}\mathbf{r}$ of the matrices $\mathbf{V}^T$,$\mathbf{V}$ with an arbitrary vector $\mathbf{r}$ amount to performing respectively a Discrete Cosine Transform of type-II (DCT-II) and an Inverse Discrete Cosine Transform of type-II (IDCT-II) [22] on $\mathbf{r}$, both of which can be computed with near-linear complexity $O(n \log n)$ (instead of the quadratic complexity $O(n^2)$ of general matrix-vector products) using Fast Fourier Transform. This is similar to a fast Poisson solver like [16] in one dimension.

By inserting (17) into (15), we arrive at the following analytical solution for stress at any given time for the pre-selected discrete points of the multi-segment line:

$$\boldsymbol{\sigma}(t) = \mathbf{V}\mathbf{L}(t)\mathbf{V}^T\mathbf{B}\mathbf{j} \tag{20}$$

where:

$$\mathbf{L}(t) = \begin{bmatrix} t & & \\ & \frac{e^{\lambda_2 t}-1}{\lambda_2} & \\ & & \ddots \\ & & & \frac{e^{\lambda_n t}-1}{\lambda_n} \end{bmatrix} \tag{21}$$

and $\lambda_j, j = 2, \ldots, n$ are given by (18).

The above enable us to construct a procedure of near-linear complexity (in the number of discretization points) for computing stress at any given time at the discretized points, which can be decomposed into initial one-time operations and the main stress calculation for the given time. This is presented in the following Algorithm 1 and Algorithm 2 respectively:

Algorithm 1: Initial Formulation

Input: parameters κ and β, discretization step Δx, vector of segment intersection coordinates $\mathbf{l} = [l_1, \ldots, l_m]^T$ ($l_m \equiv L$ equals the line length), vector of segment current densities $\mathbf{j} = [j_1, \ldots, j_m]^T$

Output: vector of eigenvalues $\boldsymbol{\lambda}$, intermediate vector $\mathbf{x}$

1. # of discretization points $n = \frac{L}{\Delta x}$
2. Construct $\mathbf{B} = \frac{\kappa\beta}{\Delta x}\mathbf{D}$, with $\mathbf{D}$ as in (11)
3. Calculate $\mathbf{r} = \mathbf{B}\mathbf{j}$
4. Perform DCT-II on vector $\mathbf{r}$ to obtain intermediate vector $\mathbf{x}$
5. Compute eigenvalues $\boldsymbol{\lambda} = [0, \lambda_2, \ldots, \lambda_n]^T$ from (18)

Algorithm 2: Transient Stress Calculation

Input: vector of eigenvalues $\boldsymbol{\lambda} = [0, \lambda_2, \ldots, \lambda_n]^T$, intermediate vector $\mathbf{x}$, time t

Output: vector of EM stress $\boldsymbol{\sigma}(t)$ at the discretized points at time t

1. Form the diagonal matrix $\mathbf{L}$(t) for the given time t from (21)
2. Calculate $\mathbf{q} = \mathbf{L}(t)\mathbf{x}$
3. Perform IDCT-II on vector $\mathbf{q}$ to obtain the final vector $\boldsymbol{\sigma}(t)$ of EM stress at time t

Complexity Analysis. Algorithm 1 has an one-time cost since it only needs to be executed once in order to compute matrices that are time-invariant. The two most computationally expensive steps of the algorithm are the calculation of vector $\mathbf{r}$ in Step 3 and the DCT-II of $\mathbf{r}$ in Step 4, which have asymptotic complexity $O(nm)$ and $O(n \log n)$ respectively. Since typically $m \ll n$, the algorithm is near-linear in n.

In Algorithm 2, both Step 1 and Step 2 are $O(n)$ since $\mathbf{L}$ is a diagonal matrix, while the IDCT-II has computational complexity of $O(n \log n)$. Thus, Algorithm 2 has also asymptotic complexity $O(n \log n)$ and is near-linear in n.

To take it a step further, if the proposed method is applied on a complete power grid for EM analysis, Algorithm 2 can be executed entirely in parallel for the different lines of the power grid (task-level parallelization), since each line can be handled independently as remarked in Section 2. Furthermore, a large amount of data-level parallelization is included in the formulation of matrix $\mathbf{L}(t)$ as well as the DCT-II/IDCT-II computational kernels.

4 NUMERICAL RESULTS

In this section, we present our numerical results in order to validate the proposed analytical method of Section 3. The first part of the experimental evaluation consists of a proof-of-concept trial using an artificial five-segment line, which is described in Section 4.1. Then, in Section 4.2, we employ our method on the publicly-available IBM Power Grid [23] (IBMPG) benchmarks in order to illustrate the applicability of our method in large-scale designs. For all benchmarks, we assume them to be Cu DD interconnects in order to ensure the separate analysis of each layer and of each line of the power grid.

For all experiments, the proposed method was implemented [2] in MATLAB R2021a and was compared to the industrial FEM-based tool, COMSOL. The specifications for this technology are listed in Table 1. Finally, all the above were run on a Windows machine with 32GB memory and a 3.6GHz i7 processor with 4×8 cores.

4.1 Artificial 5-Segment Line

For the first experiment, we have created an artificial straight-line benchmark of total length $100\mu m$ with five segments of $20\mu m$, $25\mu m$, $15\mu m$, $10\mu m$ and $20\mu m$ with corresponding constant current densities of $-2 \times 10^{10}\ A/m^2$, $1 \times 10^{10}\ A/m^2$, $1.5 \times 10^{10}\ A/m^2$, $-1 \times 10^{10}\ A/m^2$ and $0.5 \times 10^{10}\ A/m^2$.

[2] Github repository: https://github.com/oaxelou/EM_analytical

Table 1: Cu DD interconnect typical values for transient EM simulation [24].

Symbol	Physical quantity	Value
e	Electron charge	1.609×10^{-19} C
ρ	Electrical resistivity	$2.25 \times 10^{-8} \Omega$ m
$Z*$	Effective charge number	1
Ω	Atomic volume for the metal	$1.182 \times 10^{-29} m^3$
D_0	Diffusivity constant	$1.3 \times 10^{-9} m^2/s$
B	Bolk modulus for the metal	28 GPa
k_B	Boltzmann's constant	1.3806×10^{-23} J/K
T	Temperature	378K

Taking into consideration the lifetime of modern circuits, we demonstrate the stress build-up at $t = 6.38 \times 10^8$s, which corresponds to 20 years, as well as at $t = 10^7$s and $t = 10^8$s. We compare the results of our method with COMSOL and use as discretization step $\Delta x = 1\mu m$. As can be seen in Fig. 4, our method matches almost perfectly well with the COMSOL simulation, with relative error well below 0.5%, without the need for denser discetization.

However, it needs to be pointed out that since COMSOL discretizes the space coordinate using FEM techniques, the correspondence between our FDM-discretized space and COMSOL can vary. This problem is more pronounced in larger circuits with fine discretization where the error that is added, due to the approximation of FDM by FEM methods, is accumulated and affects both the correspondence on the x axis (the spatial points) as well as the value of stress at those points, since it is spatially dependent.

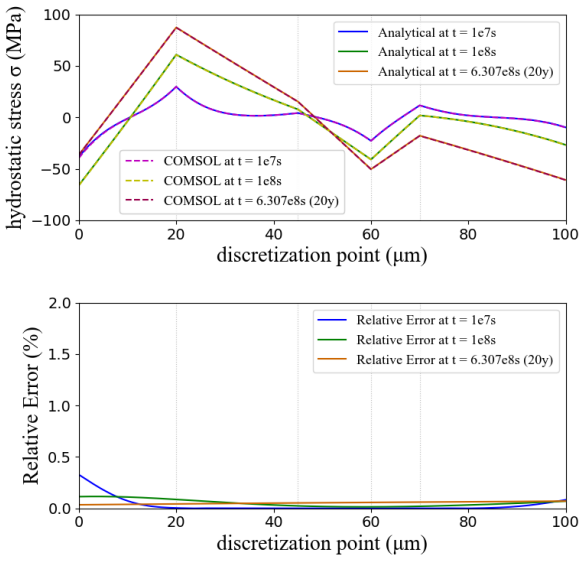

Figure 4: (top) Accuracy comparison of our proposed method with COMSOL on an artificial 5-segment line at $t = 1e7s$, $t = 1e8s$ and $t = 20$ years, and (bottom) their relative errors.

Table 2: IBM Benchmarks Characteristics.

IBMPG Benchmark	#lines	avg. line length (m)	total #segm	avg. #segm. per line
IBMPG1	1717	0.00540	29750	17.33
IBMPG2	1271	0.00532	125668	98.87
IBMPG3	7640	10.37635	835071	109.30
IBMPG4	5160	0.00762	932492	180.72
IBMPG5	3840	0.01149	1076571	280.36
IBMPG6	8521	3.01821	1648621	193.48

4.2 IBM Power Grid Benchmarks

In this section, we employ our method on the large publicly available IBM benchmarks in order to prove the scalability of our method.

In Table 2, we provide the characteristics of the IBM benchmarks. More specifically, column *#lines* describes the total number of lines of each power grid; *avg. line length* describes the average length of the lines; *total #segm* provides information on the total number of segments on the power grid and *avg. #segm. per line* offers an average value of the segments that compose a line of the corresponding power grid.

For this experiment, we performed EM stress analysis on the whole power grid at $t = 20$ years using our method and compared our results with the FEM-based solver, COMSOL. We analyze each line separately and independently and as the number of segments might be slightly different, we report the the average runtime per line. For both methods, the discretization step was set to the same value. However, and as was mentioned in Section 4.1, due to the FEM approximation of FDM, we expect an error, especially for the larger benchmarks. Moreover, and as a consequence of the large runtimes of the latter, we only ran COMSOL on a number of representative lines. We collected the average value of the above-mentioned results in Table 3. In particular, in column *avg length* we provide the average length of the lines of the corresponding power grid; *avg #segm* is the average number of segments of the lines; *discr. step* is the discretization step for the spatial coordinate and *avg #discr points per line* is the average number of the resulting discretization points on the lines of the power grid. Then, we provide the average runtimes of our method and the corresponding average runtimes of COMSOL, as well as the speedup that our method achieved.

The results show that our method can be three orders of magnitude faster than COMSOL, with speedup ranging from 25.84× to 257.6×. This high speedup is a result of many factors. First and foremost, COMSOL performs a numerical transient analysis using an adaptive timestep. It induces a large overhead to iteratively calculate the stress as a function of time since the formula needs to be evaluated in all previous time points in order to obtain the current.

In contrast, our closed-form equation directly calculates the transient stress without discretizing time, so there is no trade-off in this context between accuracy and performance no matter the point in time where we want to find the stress. Furthermore, it needs to be pointed out that the formulation time of our method is an one-time cost that doesn't need to be repeated for every time we want to perform EM stress analysis. This means, subsequently, that the proposed method can be used for both transient analysis and EM-failure test. For better understanding, we demonstrate an example of transient analysis is illustrated in Fig. 5 where we run EM stress analysis at 7 timestamps with analytical formulation time 2.27s and total execution time being 2.73s.

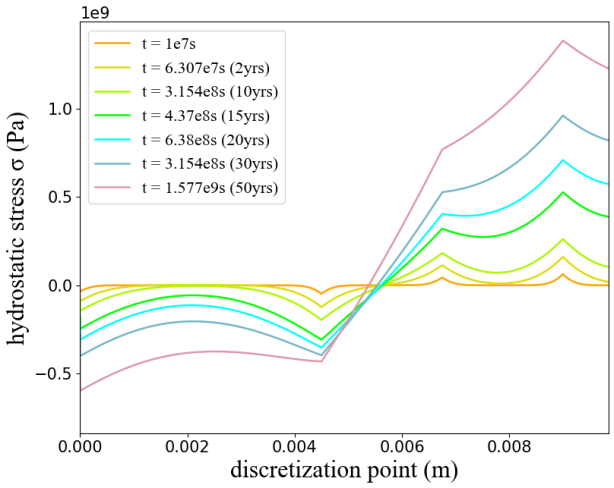

Figure 5: EM stress across a line of IBMPG1 at multiple times using the proposed method.

Finally, all of the above are depicted in the scalability of the two methods under test. On the one hand, the runtimes of COMSOL tend to follow an exponential pattern which does not permit the method to be applied on large scale circuits, hence our limitation in the number of lines that we could test. On the other hand, and by observing the results, one can comprehend the almost linear complexity of our methodology, which was proven in Section 3.

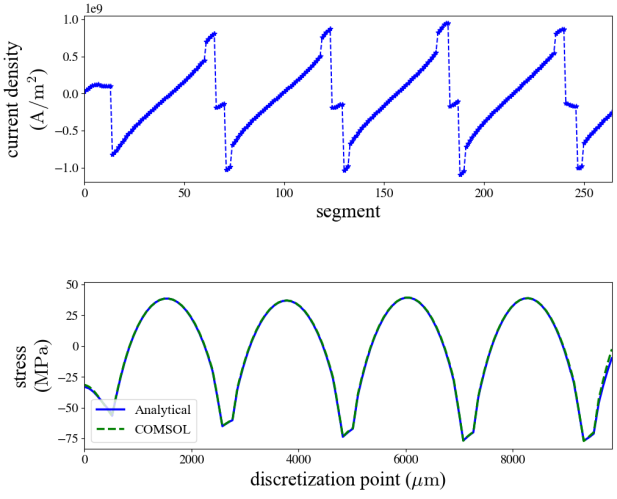

Figure 6: (top) Current density profile of an IBMPG5 benchmark line, and (bottom) comparison of the corresponding stress across the line at $t = 20$ years using the proposed method and COMSOL.

Table 3: Runtime comparison of proposed methodology with COMSOL on IBMPG Benchmarks at $t = 20$ years.

Power Grid Benchmark	discr. step (μm)	avg #discr points per line	Proposed semi-Analytical methodology			COMSOL	
			Formulation time (s)	Execution time (s)	Total time (s)	Time (s)	Speedup
IBMPG1	1	5396.35	2.92289	0.41958	3.34247	86.38134	25.84×
IBMPG2	1	5318.33	0.63518	0.10559	0.74077	70.53742	95.22×
IBMPG3	1000	10377.81	6.40641	1.31453	7.72094	1474.84011	191.02×
IBMPG4	1	7620.81	1.81713	0.27706	2.09419	466.86929	222.94×
IBMPG5	1	11492.19	3.24564	0.56583	3.81147	325.79535	85.48×
IBMPG6	400	7546.93	5.02081	0.83445	5.85526	1508.34254	257.6×

In addition to the performance scalability, in Fig. 6, we provide a comparison on accuracy between the proposed method and COMSOL on a line of IBMPG5 benchmark at $t = 20$ years with the same discretization step as depicted in Table 3. It is easily noticeable that the EM analysis is almost indistinguishable across all points.

5 CONCLUSION

In this paper, we proposed a fast semi-analytical approach for the solution of the EM hydrostratic stress at discrete spatial points in multi-segment lines of power grids. Our method creates a formula which can be used to independently provide the value of stress at any time. More specifically, our method takes advantage of the specific tridiagonal form of the system matrix whose eigenvalues and eigenvectors are known in advance and creates a closed-form equation with almost linear time complexity that is very easily parallelizable. The resulting equation can be used for transient analysis of the EM stress. Experimental results of our method on the large scale IBM benchmarks, in comparison with the industrial FEM-based solver COMSOL, illustrated almost perfect agreement with the latter while being up to 258× faster. Finally, we demonstrate that, due to the excellent runtimes, our method can be efficiently employed for a complete power grid EM analysis.

ACKNOWLEDGMENTS

This research has been coâĂŘfinanced by the European Regional Development Fund of the European Union and Greek national funds through the Operational Program "Competitiveness, Entrepreneurship and Innovation", under the call "Research âĂŞ Create âĂŞ Innovate" (project code: T2EDK-00609).

REFERENCES

[1] Jens Lienig. Electromigration and its impact on physical design in future technologies. In *Proceedings of the 2013 ACM International Symposium on Physical Design*, ISPD '13, page 33âĂŞ40, New York, NY, USA, 2013. Association for Computing Machinery. ISBN 9781450319546.

[2] C.-C. Yang, T. Spooner, P. McLaughlin, C.K. Hu, H. Huang, Y. Mignot, M. Ali, G. Lian, R. Quon, T. Standaert, and D. Edelstein. Microstructure modulation for resistance reduction in copper interconnects. In *2017 IEEE International Interconnect Technology Conference (IITC)*, pages 1–3, Taiwan, 2017.

[3] Jens Lienig and Matthias Thiele. *Fundamentals of electromigration-aware integrated circuit design*. Springer International Publishing, 2018.

[4] I. A. Blech. Electromigration in thin aluminum films on titanium nitride. *Journal of Applied Physics*, 47(4):1203–1208, 1976.

[5] J.R. Black. ElectromigrationâĂŤa brief survey and some recent results. *IEEE Transactions on Electron Devices*, 16(4):338–347, 1969.

[6] Sachin S. Sapatnekar. Electromigration-aware interconnect design. In *Proceedings of the 2019 International Symposium on Physical Design*, ISPD '19, page 83âĂŞ90, New York, NY, USA, 2019. Association for Computing Machinery. ISBN 9781450362535.

[7] M. A. Korhonen, P. Bo/rgesen, K. N. Tu, and CheâĂŘYu Li. Stress evolution due to electromigration in confined metal lines. *Journal of Applied Physics*, 73(8): 3790–3799, 1993.

[8] Mohammad Abdullah Al Shohel, Vidya A. Chhabria, and Sachin S. Sapatnekar. A new, computationally efficient âĂIJblech criterionâĂİ for immortality in general interconnects. In *2021 58th ACM/IEEE Design Automation Conference (DAC)*, pages 913–918, 2021.

[9] Sandeep Chatterjee, Valeriy Sukharev, and Farid N. Najm. Power grid electromigration checking using physics-based models. *IEEE Transactions on Computer-Aided Design of Integrated Circuits and Systems*, 37(7):1317–1330, 2018.

[10] Chase Cook, Zeyu Sun, Ertugrul Demircan, Mehul D. Shroff, and Sheldon X.-D. Tan. Fast electromigration stress evolution analysis for interconnect trees using krylov subspace method. *IEEE Transactions on Very Large Scale Integration (VLSI) Systems*, 26(5):969–980, 2018.

[11] Olympia Axelou, George Floros, Nestor Evmorfopoulos, and George Stamoulis. Accelerating electromigration stress analysis using low-rank balanced truncation. In *2022 18th International Conference on Synthesis, Modeling, Analysis and Simulation Methods and Applications to Circuit Design (SMACD)*, pages 1–4, 2022.

[12] Hai-Bao Chen, Sheldon X.-D. Tan, Xin Huang, Taeyoung Kim, and Valeriy Sukharev. Analytical modeling and characterization of electromigration effects for multibranch interconnect trees. *IEEE Transactions on Computer-Aided Design of Integrated Circuits and Systems*, 35(11):1811–1824, 2016.

[13] Hai-Bao Chen, Sheldon X.-D. Tan, Jiangtao Peng, Taeyoung Kim, and Jie Chen. Analytical modeling of electromigration failure for vlsi interconnect tree considering temperature and segment length effects. *IEEE Transactions on Device and Materials Reliability*, 17(4):653–666, 2017.

[14] Mohammad Abdullah Al Shohel, Vidya A. Chhabria, Nestor Evmorfopoulos, and Sachin S. Sapatnekar. Analytical modeling of transient electromigration stress based on boundary reflections. In *2021 IEEE/ACM International Conference On Computer Aided Design (ICCAD)*, pages 1–8, 2021.

[15] Liang Chen, Sheldon X.-D. Tan, Zeyu Sun, Shaoyi Peng, Min Tang, and Junfa Mao. A fast semi-analytic approach for combined electromigration and thermomigration analysis for general multisegment interconnects. *IEEE Transactions on Computer-Aided Design of Integrated Circuits and Systems*, 40(2):350–363, 2021.

[16] Haifeng Qian and Sachin S. Sapatnekar. Fast poisson solvers for thermal analysis. In *2010 IEEE/ACM International Conference on Computer-Aided Design (ICCAD)*, pages 698–702, 2010.

[17] George A. Sullivan. Search for reversal in copper electromigration. *Journal of Physics and Chemistry of Solids*, 28(2):347–350, 1967. ISSN 0022-3697.

[18] Jeffrey Gambino. Process technology for copper interconnects. In *Handbook of Thin Film Deposition (Fourth Edition)*, pages 147–194. 2018.

[19] Sandeep Chatterjee, Valeriy Sukharev, and Farid N. Najm. Fast physics-based electromigration checking for on-die power grids. In *2016 IEEE/ACM International Conference on Computer-Aided Design (ICCAD)*, pages 1–8, 2016.

[20] Alan V. Oppenheim, Alan S. Willsky, and S. Hamid Nawab. *Signals & Systems (2nd Ed.)*. Prentice-Hall, Inc., USA, 1996. ISBN 0138147574.

[21] Konstantis Daloukas, Nestor Evmorfopoulos, Panagiota Tsompanopoulou, and George Stamoulis. Parallel fast transform-based preconditioners for large-scale power grid analysis on graphics processing units (gpus). *IEEE Transactions on Computer-Aided Design of Integrated Circuits and Systems*, 35(10):1653–1666, 2016.

[22] Charles Van Loan. *Computational Frameworks for the Fast Fourier Transform*. Society for Industrial and Applied Mathematics, USA, 1992. ISBN 0898712858.

[23] Sani R. Nassif. Power grid analysis benchmarks. In *Proceedings of the 2008 Asia and South Pacific Design Automation Conference*, ASP-DAC '08, pages 376–381. IEEE Computer Society Press, 2008. ISBN 9781424419227.

[24] S.M. Alam, C.L. Gan, F.L. Wei, C.V. Thompson, and D.E. Troxel. Circuit-level reliability requirements for cu metallization. *IEEE Transactions on Device and Materials Reliability*, 5(3):522–531, 2005.